Journal of Biomedical Optics

SPIEDigitalLibrary.org/jbo

Designing multifocal corneal models to correct presbyopia by laser ablation

Aixa Alarcón
Rosario G. Anera
Luis Jiménez del Barco
José R. Jiménez

SPIE

Designing multifocal corneal models to correct presbyopia by laser ablation

Aixa Alarcón, Rosario G. Anera, Luis Jiménez del Barco, and José R. Jiménez
University of Granada, Laboratory of Vision Sciences and ApplicationsLaboratory of Vision Sciences and Applications, Department of Optics, Edificio Mecenas, Facultad de Ciencias, Avda Fuentenueva s/n, 18071 Granada,Spain

Abstract. Two multifocal corneal models and an aspheric model designed to correct presbyopia by corneal photoablation were evaluated. The design of each model was optimized to achieve the best visual quality possible for both near and distance vision. In addition, we evaluated the effect of myosis and pupil decentration on visual quality. The corrected model with the central zone for near vision provides better results since it requires less ablated corneal surface area, permits higher addition values, presents stabler visual quality with pupil-size variations and lower high-order aberrations. [DOI: 10.1117/1.JBO.17.1.018001]

Keywords: refractive surgery; multifocal ablations; presbyopia corrections; pseudo-accommodation; visual quality.

Paper 11516 received Sep. 16, 2011; revised manuscript received Nov. 9, 2011; accepted for publication Nov. 9, 2011; published online Feb. 6, 2012.

1 Introduction

Presbyopia is the refractive condition in which the accommodative ability of the eye is insufficient for near vision. Given that this condition is inevitable with aging, treatment becomes even more important as the population ages. Different compensation methods are available, including spectacles or contact lenses,[1] intraocular lenses,[2] scleral spacing procedures,[3] corneal inlays,[4] conductive keratoplasty,[5] and excimer laser-based approaches.[6] However, the correction of presbyopia is difficult because of the dynamic nature of accommodation.

Corneal ablation by laser has become a steadily more common treatment for presbyopic patients.[7–19] Currently, clinics offer mainly two techniques for presbyopia treatment: monovision and multifocal corneal ablation. In monovision, one eye is corrected for distance (normally the dominant eye) while the other eye is corrected for near vision (the nondominant eye).[15–19] Some authors recommend, furthermore, that asphericity of the corrected cornea be incremented for near vision (hyperprolate cornea) to increase spherical aberration and thereby provide greater depth of field.[20] Despite the degree of satisfaction of patients subjected to monovision correction by LASIK (between 88 and 98%),[15–17] studies demonstrate a reduction in the contrast-sensitivity function, a loss of visual-discrimination capacity, and a clear worsening of stereoacuity, among other functions.[18,19] In multifocal ablations, the aim is to achieve a multifocal cornea able to correct any visual defect for distance while simultaneously reducing spectacle dependency for near vision. There are two main patterns of multifocal ablations. The first, known as central presbyLASIK, consists of creating a central hyperpositive zone, designed to provide near vision, leaving the mid-peripheral cornea for distance vision.[7–9] The other group, known as peripheral presbyLASIK, corrects the mid-peripheral zone for near vision,[10–14] leaving the center corrected for distance vision. For both multifocal treatments, the results are satisfactory, although some studies report diminished contrast sensitivity;[8] increases in coma, trefoil, and total higher-order aberrations;[10] or decreases in best spectacle-corrected visual acuity.[8,9,11] It would be useful to delve into the causes of this loss of visual quality as well as to investigate the theoretical differences between the corneal-ablation models most widely used in the clinic: an aspheric model (similar to the one proposed in monovision for expanding the depth of field in the corrected eye for near vision, optimizing the Q value) and two multifocal models (a central model and a peripheral model). In this work, each model was optimized with the aim of achieving the best visual quality possible both in near and distance vision. In addition, we evaluated the effect that pupil size and its decentration has on the visual quality provided by these models.

2 Methods

We used the Liou-Brennan model[21] to represent our unaccommodated emmetropic eye, as it has been demonstrated to be a useful model to evaluate the optical quality by varying only the anterior surface of the cornea.[22,23] The calculations were performed using the ZEMAX-SE Optical Design Program (ZEMAX Development Corp., Bellevue, Washington, USA) at a wavelength of 555 nm.

2.1 *Metric to Evaluate the Visual Quality: Neural Sharpness*

Although there are many metrics to evaluate retinal image quality, some of the most commonly used, such as the root-mean-square (RMS) wavefront error and the Strehl ratio, show low correlation with subjective performance.[24,25] Given that the objective of the present work is to simulate the visual quality of a subject treated with a multifocal ablation, we

Address all correspondence to: Aixa Alarcon, Laboratory of Vision Sciences and Applications, Department of Optics, Edificio Mecenas, Facultad de Ciencias, Avda Fuentenueva s/n 18071 Granada, Spain. Tel: 34 605036387; Fax: 34 958248533; E-mail: aixaalarcon@ugr.es

0091-3286/2012/$25.00 © 2012 SPIE

selected a metric that provides a good description of the subjective image quality: the Neural Sharpness metric.[25] Neural Sharpness was introduced as a way to capture the effectiveness of a Point-Spread Function (PSF) for simulating the neural portion of the visual system. This metric can be defined as:[26]

$$\mathrm{NS} = \frac{\int_{\mathrm{psf}} \mathrm{PSF}(x,y)\, g(x,y)\, \mathrm{d}x\, \mathrm{d}y}{\int_{\mathrm{psf}} \mathrm{PSF}_{\mathrm{DL}}(x,y)\, g(x,y)\, \mathrm{d}x\, \mathrm{d}y} \quad (1)$$

where $g(x,y)$ is a bivariate-Gaussian function with a standard deviation of 1 arcmin, which represents a neural weighting function, and the $\mathrm{PSF}_{\mathrm{DL}}(x,y)$ is the diffraction-limited PSF. Neural Sharpness, which combines the eye's optics and neural blur, has been demonstrated to be effective for assessing visual performance.[25] Furthermore, this metric provides a single number that describes the subjective impact of each patient's wave aberration, making it especially useful for the purposes of this study.

2.2 *Corneal Models*

Our interest is to optimize the design of three corneal models: two multifocal models (the central model and the peripheral model) and an aspheric model. To design the aspheric model, we looked for an aspheric corneal surface, characterized by a curvature radius (R_c) and asphericity (Q_c) of 6.5 mm in diameter.[19] This area is joined to the original cornea of the Liou-Brennan model by a transition surface of 9.5 mm in diameter.

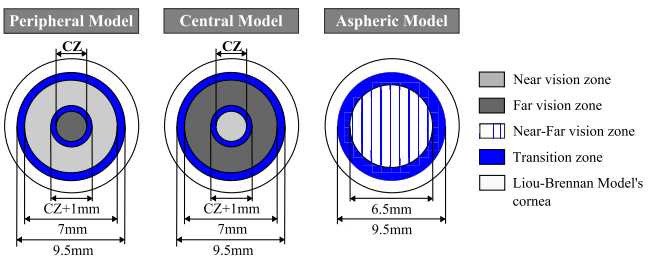

Fig. 1 Design of the three corneal models: peripheral model (left), central model (center), and aspheric model (right). The central zone (CZ) and the dimensions of the different zones are represented for each model.

To design the multifocal corneal models, we divided the cornea into three main zones, as shown in Fig. 1. The central zone (CZ) is a conical surface for which the diameter, curvature radius (R_c), and asphericity (Q_c) are variables that we wish to optimize. The peripheral zone is also characterized by a conicoid with a curvature radius (R_p) and asphericity (Q_p) that are also optimized for each model. The thickness of the transition zone between the central zone and the peripheral zone is 0.5 mm.[23] The peripheral zone has a diameter of 7 mm and is joined to the original cornea of the Liou-Brennan model by a transition surface of 9.5 mm in diameter.[13] The transition zones are represented by a third-degree polynomial given by the equation $z(w) = a_0 + a_1 w + a_2 w^2 + a_3 w^3$, where the parameters a_0, a_1, a_2, and a_3 are determined considering the function and its first derivative continuous at the intersection points. On this basis, we designed the three corneal models (see Fig. 1):

- The peripheral model (PM) is a multifocal cornea with a central zone created for distance vision and the mid-peripheral cornea zone for near vision.
- The central model (CM) is a multifocal cornea with a central zone created for near vision, leaving the mid-peripheral cornea for distance vision.
- The aspheric model (AM) is a cornea with a conical central zone designed to provide simultaneously near and distance vision.

The optimization process (Fig. 2) in all cases was carried out for a pupil diameter of 4 mm. First, we calculated the radius and the asphericity of the cornea that minimized the RMS wavefront error for distance vision (object situated 6 m from the anterior corneal surface) and for near vision. Because the addition used in the clinic varies according to the subject and the technique used,[8,12] we considered two different addition values: $+1D$ and $+2.5D$.[13] To simulate these additions, we situated the object in near vision at two distances from the corneal surface: 0.4 m ($+2.5D$) and 1 m ($+1D$). The RMS was evaluated with respect to the centroid (the point that minimizes the variance of the wavefront). Following the recommendation procedure by ZEMAX (Zemax User's Guide, April 4, 2006), we found that a sampling pattern based on the Gauss quadrature rule, with three rings and six arms, provided an accurate computation. In the central model, we formed the central zone with the radius and asphericity established by optimizing the near vision, while

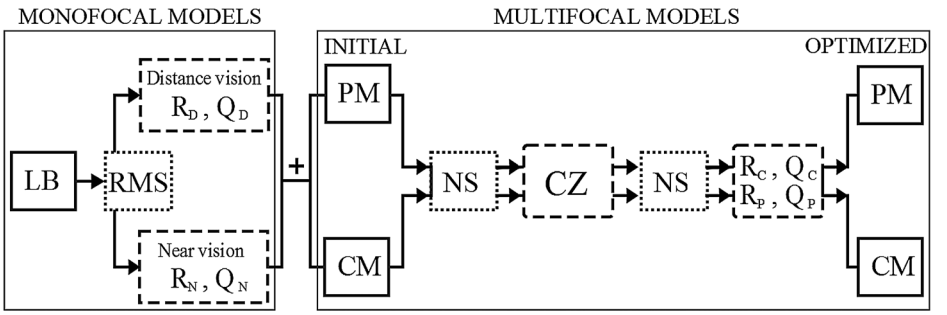

Fig. 2 Flow diagram of the optimization process followed for the optimization of the models. The boxes with the solid lines indicate the models (LB, Liou-Brennan model; PM, peripheral model; and CM, central model). The boxes with the dotted lines indicate the metric used in the optimization (RMS, root-mean-square of the wavefront error; NS, Neural Sharpness). The boxes with the broken line indicate the results of the optimization [central-zone diameter (CZ); and curvature radius and asphericity for near vision (R_N, Q_N), for distance vision (R_D, Q_D), for the central zone (R_C, Q_C), and for the peripheral zone (R_P, Q_P)].

for the peripheral zone we used the parameter determined for distance vision. In the peripheral model, we did the opposite. That is, we used the RMS to determine the initial parameters and thereby set the range of values of the curvature radius and asphericity to be evaluated. For the rest of the optimization process, we used Neural Sharpness to ensure a more precise adjustment of the parameters calculated.

After determining the radius and the asphericity of each zone and model, we determined the optimal size of the central zone. For this, we varied the CZ between 2 and 3.5 mm, choosing the diameter that provides the same Neural Sharpness for near and distance vision. After establishing the optimal size of the central zone, we re-optimized the radius and the asphericity of the central and peripheral zones (R_c, Q_c, R_p, and Q_p). This re-optimization was undertaken by iteratively varying the value of these parameters and calculating for each case the visual quality by the Neural Sharpness. This re-optimization was necessary because to get the initial values R_c, Q_c, R_p, and Q_p by ZEMAX, we did not take into account the multifocal nature of the cornea (since the optimization was made for a general conical cornea). Therefore, on integrating all these values and forming the multifocal surface, it was necessary to recalculate these parameters to improve the resulting visual quality.

To determine the parameters that characterize the aspheric model (R_c and Q_c), we began with the original values of the Liou-Brennan model and we iteratively varied both parameters until finding a better relation between near and distance vision. Given that the aim of this model is to achieve a more curved corneal surface in the center and flatter at the periphery (thereby improving near vision for small pupils while maintaining distance vision for large pupils), we used a pupil of 4 mm to evaluate distance vision and 2 mm to evaluate near vision. The transition zone was fit by a third-degree polynomial in a way similar to that used in multifocal models.

Once all the parameters that provide the best near and distance vision were set for each of these corneal models, we calculated the ablation depth that would involve applying each of them to the cornea of the emmetropic eye of the Liou-Brennan model. To compare visual quality, we also assessed the effect of the pupil size and its decentration in Neural Sharpness for near and distance vision. In addition, we compared the spherical aberration, $Z(4,0)$, and the higher-order aberrations for a 5-mm pupil size.

3 Results

3.1 *Design and Optimization of the Corneal Models*

Figure 3 presents the Neural Sharpness (NS) for near and distance vision according to the central-zone size for PM and CM and for an addition of $+2.5D$[Fig. 3(a)] and $+1D$ [Fig. 3(b)]. We found an optimal central-zone size of 2.9 mm for the PM and 2.4 mm for the CM, considering an addition of $+2.5D$; and of 3 mm for the PM and 2.7 mm for the CM with an addition of $+1D$ (Table 1). This means that the CM requires a smaller central zone than that of the PM. In both models, on increasing the addition, the optimal size of the central zone decreased. Therefore, for smaller additions, the central zone of the multifocal model can be larger.

Figure 4(a) shows the NS in near and distance vision for different asphericity values ($Q = -0.3$, -0.4, -0.5, and -0.6) and for different curvature radii, considering an addition of $+2.5D$. We note that the resulting models were invariably monofocal, that is, we could improve distance and near vision, but not both at the same time. We also found that on giving the most negative values to asphericity, the maximum NS for distance vision diminished, without improving the visual quality of the near vision. The same occurred with the maximum value of the NS for near vision, although this decrease was less significant. This signifies that it is not possible to find a set of parameters that provides acceptable near and distance vision simultaneously and, therefore, it was not possible to use the aspheric model to correct $+2.5D$ of addition.

When we considered an addition of $+1D$ [Fig. 4(b)], the maximums of the curves were nearer together. Therefore, it is possible to find an R and Q that give high values of NS for near

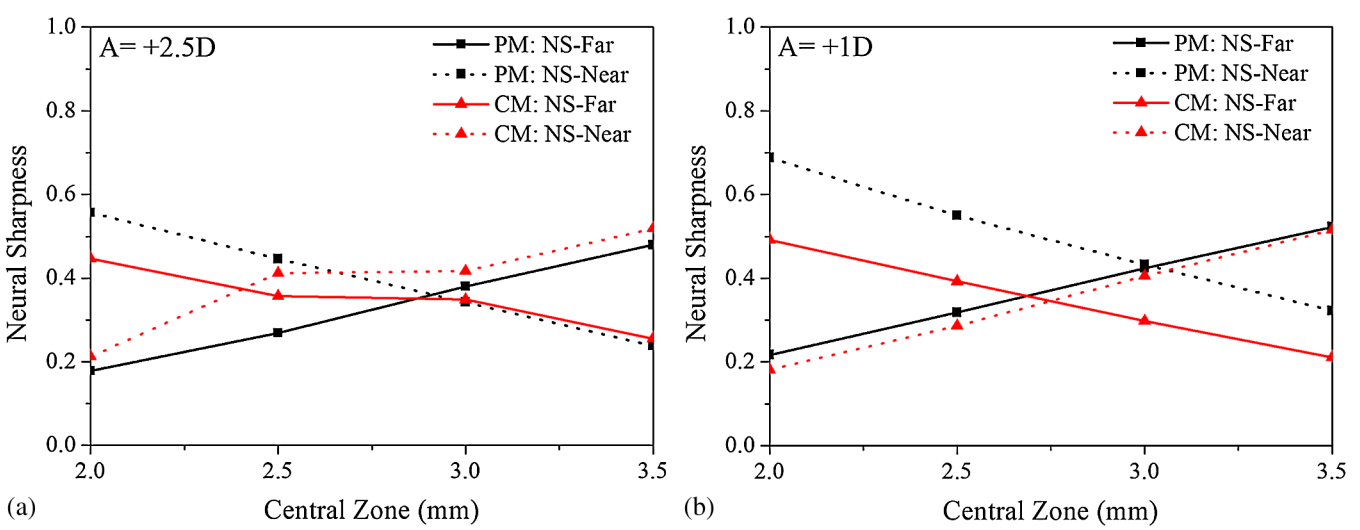

Fig. 3 Neural Sharpness for near (NS-Near) and (NS-Far) vision as a function of the central zone diameter for the peripheral model (PM) and the central model (CM). (a) Near addition power (A): $+2.5D$. (b) Near addition power (A): $+1D$.

Table 1 Results of the optimization of each model: peripheral model (PM), central model (CM), and aspheric model (AM).

Model	Addition (D)	CZ (mm)	R_c (mm)	Q_c	R_p (mm)	Q_p
PM	+2.5	2.9	7.71	−0.6	7.41	−0.27
PM	+1	3	7.68	−1	7.61	−0.28
CM	+2.5	2.4	7.36	−1	7.74	−0.26
CM	+1	2.7	7.63	−0.6	7.76	−0.21
AM	+1	—	7.67	−0.4	—	—

and distance vision simultaneously. Given that the aim is to optimize both near and distance vision, we chose the R value that provided the same NS for near and distance vision. In addition, we chose $Q = -0.4$ because it was the corneal asphericity that provided the highest NS for near and distance vision simultaneously.

Table 1 shows the parameters that optimize each of the models: PM, CM, and AM. The most striking of these results is that the central zone of the multifocal models has very negative asphericities, equal to or greater than −0.6. However, the same does not occur in the peripheral zone. The effect of the value of the addition in R_c, Q_c, R_p, and Q_p was different according to the model, while, as commented above, the optimal CZ was lower the greater the addition. For the AM, we found that the optimal radius was very similar to that found for the PM with addition of $+1D$ in its central zone, although its asphericity was lower than the asphericities found for the central zone in the two multifocal models.

We calculated the average asphericity Q (for 6 mm in diameter) that best fits each of these models. Figure 5 shows similar asphericity values in CM and AM for $+1D$ of addition. However, for the PM, the average value found was positive. This indicates that despite the PM having a larger central zone than that of the CM and with negative asphericity values, on average the final form of this multifocal cornea was oblate, that is, flatter in the center and more curved on the periphery.

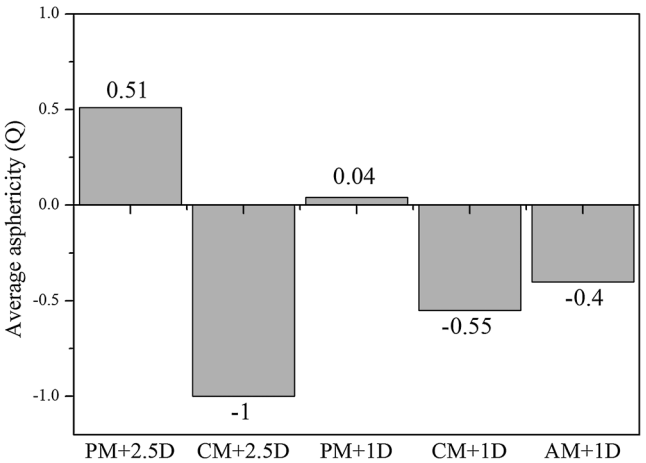

Fig. 5 Average asphericity calculated for 6 mm of diameter for the peripheral model with an addition of $+2.5D$ (PM + 2.5D), the central model with an addition of $+2.5D$ (CM + 2.5D), the peripheral model with an addition of $+1D$ (PM + 1D), the central model with an addition of $+1D$ (CM + 1D), and the aspheric model with an addition of $+1D$ (AM + 1D).

In the two multifocal models, on decreasing the near addition power, the average asphericity took values closer to zero.

3.2 *Ablation Profiles*

Figure 6(a) represents the ablation profiles associated with each of the optimized models considering an addition of $+2.5D$. As we see, the PM requires a considerably greater ablation depth. Given that we are considering an emmetropic eye in distance vision, this model leaves the central zone of the cornea almost intact, most of the ablation occurring in the mid-peripheral zone (between approximately 1.5 and 4.5 mm of radius), which is the zone corrected for near vision. In the CM, the mid-peripheral zone corrected for distance vision is also clearly distinguished, presenting an almost constant ablation depth in this zone. Figure 6(b) shows the ablation profiles for $+1D$ of addition. As might be expected, a lower addition implies less ablation depth. This reduction is very significant in the PM, although it continues to be the model that requires the greatest ablation

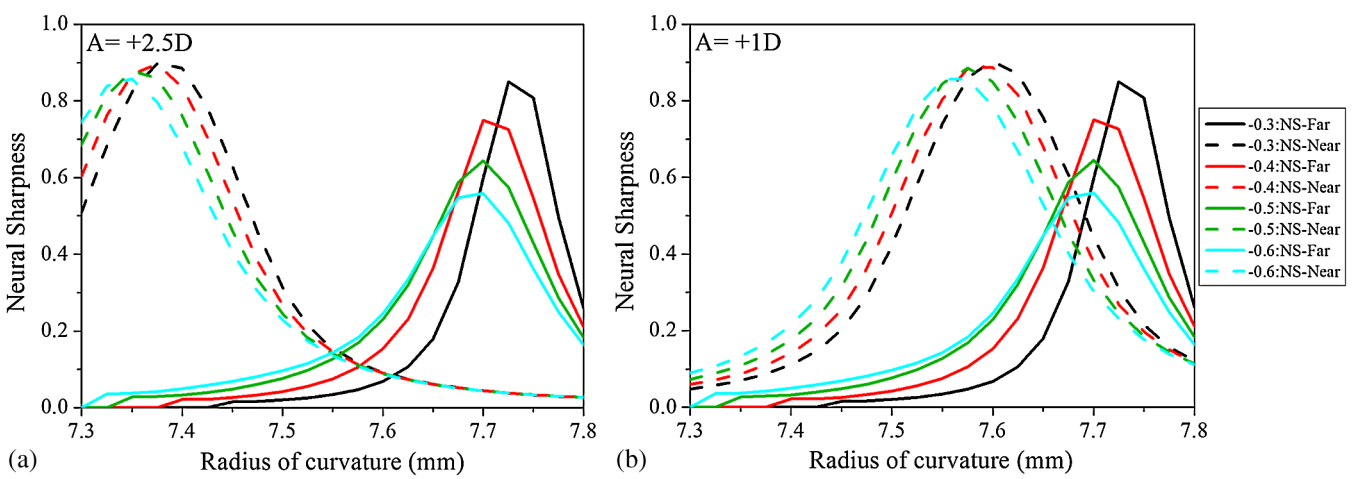

Fig. 4 Neural Sharpness for near (NS-Near) and distance (NS-Far) vision as a function of the radius of curvature and the asphericity ($Q = -0.3$, −0.4, −0.5, and −0.6) for the aspheric model. (a) Near addition power (A): $+2.5D$. (b) Near addition power (A): $+1D$.

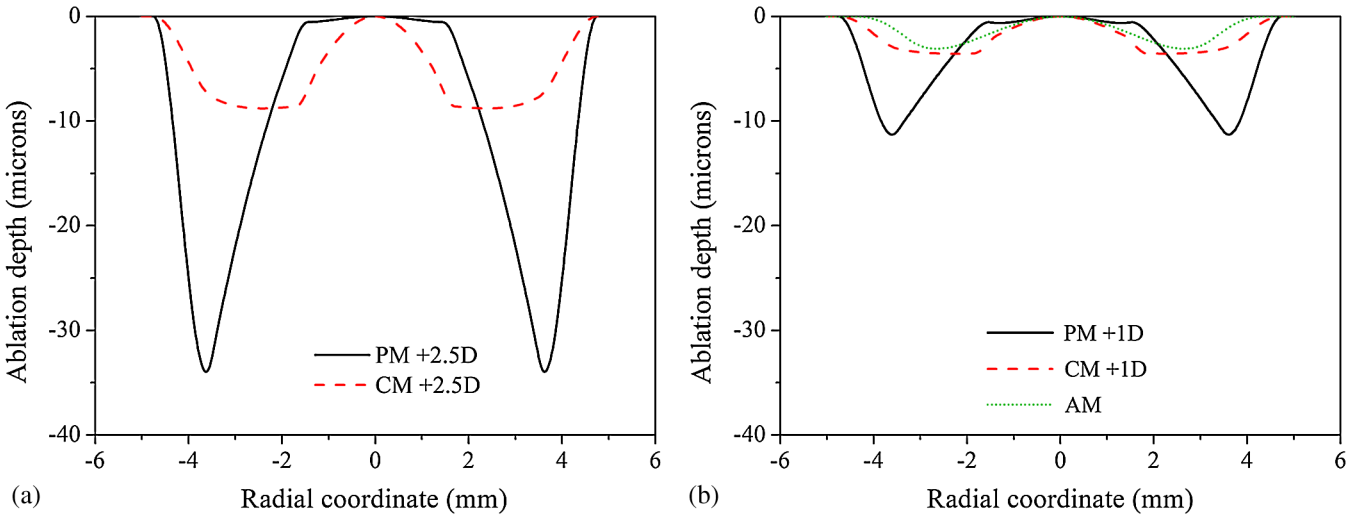

Fig. 6 Ablation profile for the different corneal models: the peripheral model (PM), the central model (CM) and the aspheric model (AM). (a) Near addition power +2.5*D*. (b) Near addition power +1*D*.

depth. The CM presents a profile very similar to that found for +2.5*D*, although, as expected, the curvature change of the central zone was less for a lower addition. The AM presented an ablation profile quite similar to that of CM, and furthermore, this was the model that required the lowest ablation depth.

3.3 *Evaluation of Visual Quality*

Figure 7 presents the NS for near and distance vision as a function of pupil diameter for the PM and CM with an addition of +2.5*D* [Fig. 7(a)] and for the PM, CM, and AM with an addition of +1*D* [Fig. 7(b)]. As expected for the multifocal models, as the pupil size enlarged, visual quality corresponding to the central corneal zone worsened, while vision corresponding to the peripheral corneal zone improved. Therefore, small pupils favored near vision in the CM but distance vision in the PM, while large pupils (>4 mm) favored distance vision in the CM and near vision in the PM, both for +2.5*D* as well as for +1*D* of addition. However, we found that for +1*D* of addition, the NS was consistently greater in both multifocal models. In addition, for +1*D*, the changes in pupil size provide less variation in the NS for vision corresponding to the peripheral corneal zone, especially for the CM. On the other hand, the CM provides higher NS for vision corresponding to the central corneal zone for all pupil sizes. However, for the vision corresponding to the peripheral corneal zone, this difference depended on the value of the addition as well as the pupil size. When we examined the AM, we found that for very small pupils, near vision was significantly improved, although for pupils larger than 3 mm, the NS of near vision was consistently worse than for the multifocal models. The NS of distance vision in the AM was very similar to that calculated for the PM for all the pupil sizes.

Figure 8 shows the effect of decentration of the pupil in the NS corresponding to each model. For the PM [Fig. 8(a) and (b)], we found that a centered pupil favors distance vision for small pupils (<4 mm). For large pupils, the NS in distance vision was practically independent of the decentration of the pupil. However, the NS for near vision was greater when the pupil was nasally decentered, regardless of size. In the CM [Fig. 8(c)

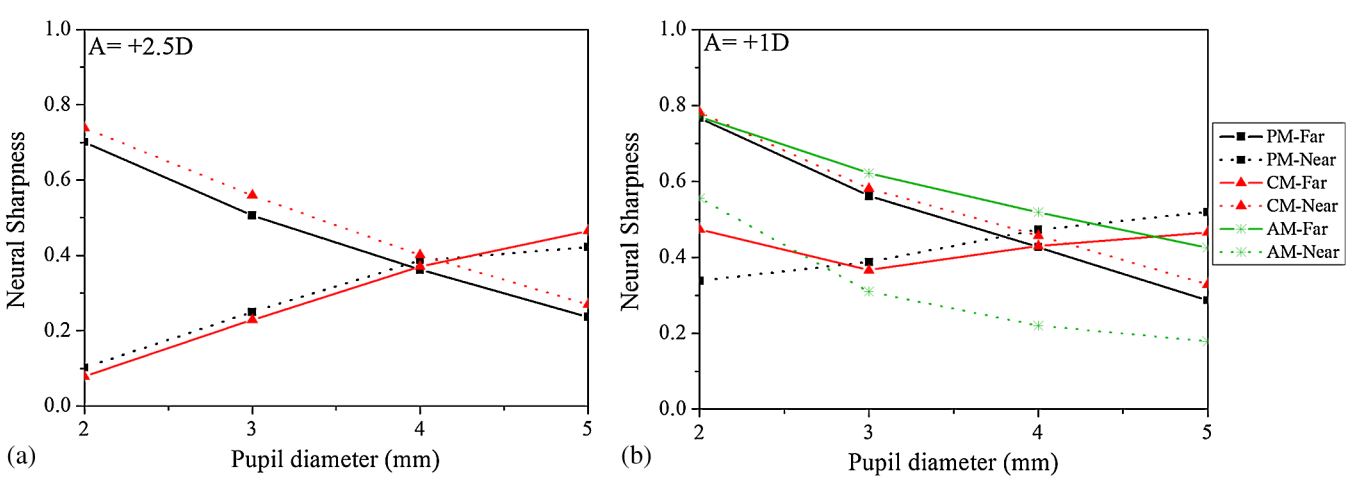

Fig. 7 Neural Sharpness for near (Near) and distance (Far) vision for different pupil sizes corresponding to the peripheral model (PM), the central model (CM), and the aspheric model (AM). (a) Near addition power (*A*): +2.5*D*. (b) Near addition power (*A*): +1*D*.

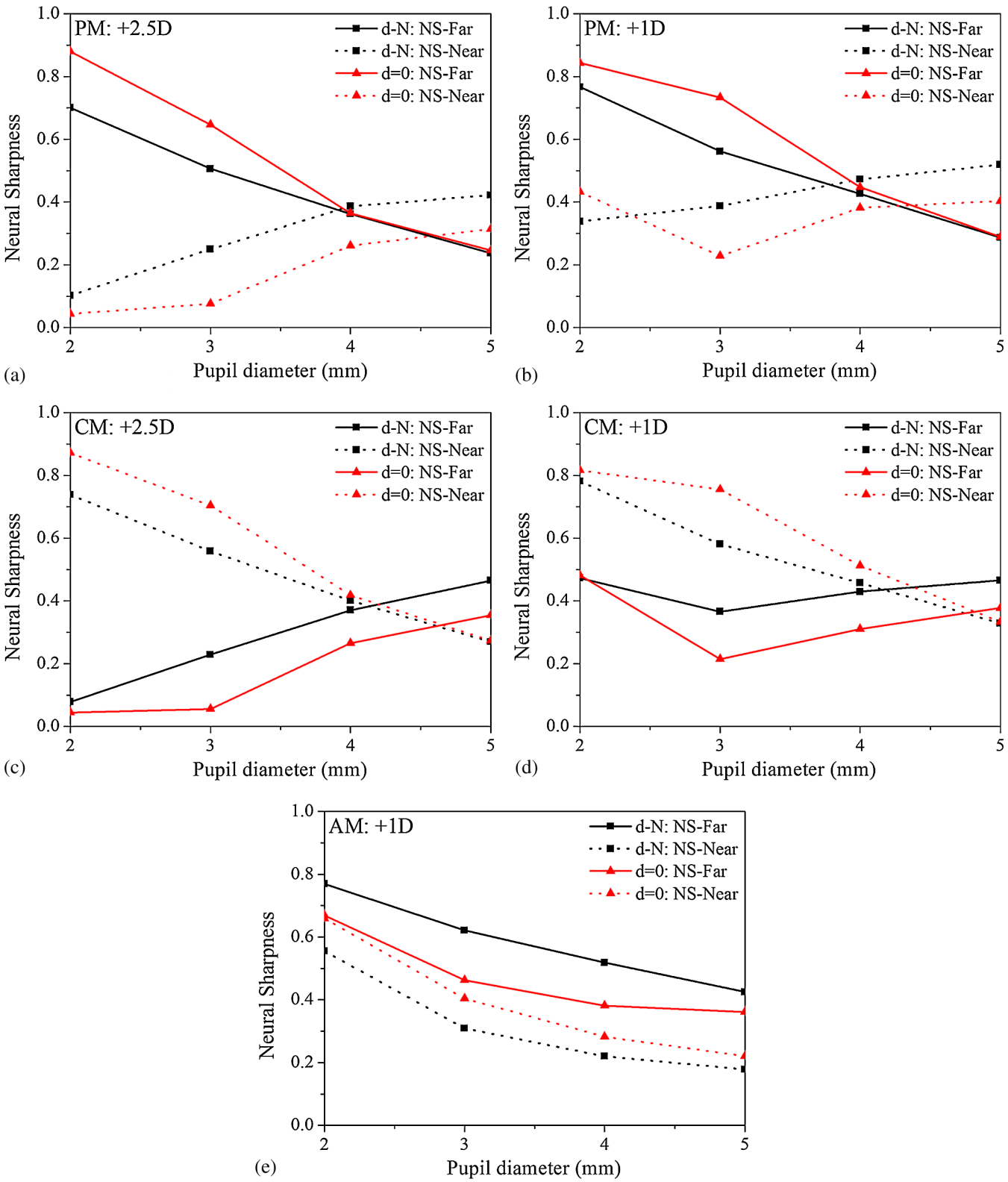

Fig. 8 Neural Sharpness for near (NS-Near) and distance (NS-Far) vision for different pupil diameter and two different positions of the pupil: centered on the optical axis ($d = 0$) and decentered nasally 0.5 mm (d-N). (a) Values found for the peripheral model (PM) with an addition of $+2.5D$. (b) Values found for the peripheral model (PM) with an addition $+1D$. (c) Values found for the central model (CM) with an addition of $+2.5D$. (d) Values found for the central model (CM) with an addition of $+1D$. (e) Values found for the aspheric model (AM) with an addition of $+1D$.

and (d)] the effect of decentering the pupil was similar to that of the PM but in the opposite way. That is, a nasal decentering of the pupil favored distance vision, while a centered pupil favored near vision. However, contrary to what occurred in other models, for $+1D$ of addition and a pupil of 2 mm, the decentration of the pupil did not alter the value of the NS in

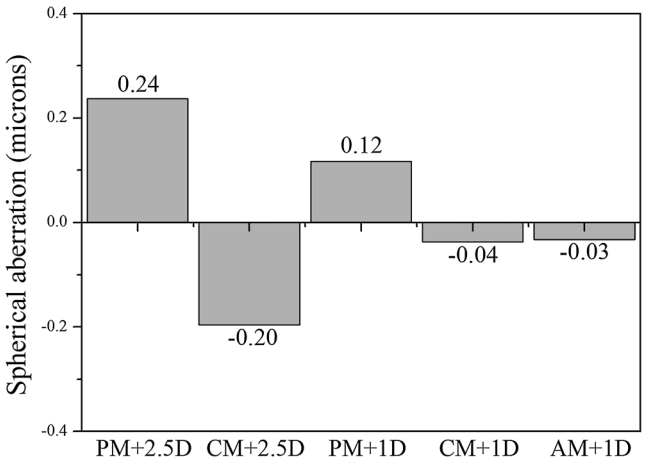

Fig. 9 Spherical aberration calculated for the peripheral model with an addition of $+2.5D$ (PM + 2.5*D*), the central model with an addition of $+2.5D$ (CM + 2.5*D*), the peripheral model with an addition of $+1D$ (PM + 1*D*), the central model with an addition of $+1D$ (CM + 1*D*), and the aspheric model with an addition of $+1D$ (AM + 1*D*).

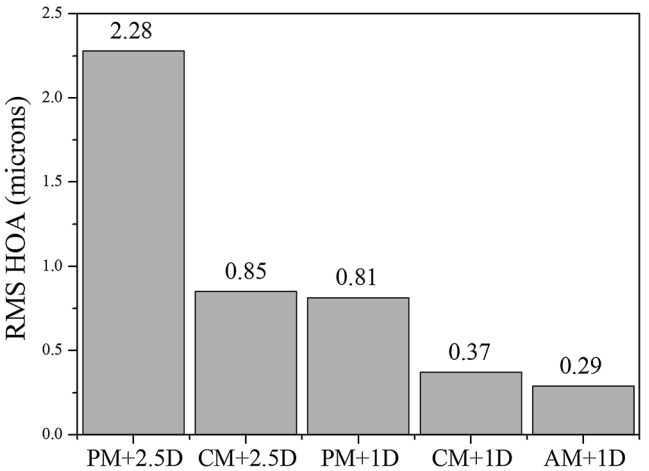

Fig. 10 Root-mean-square of higher-order aberration values (RMS HOA) calculated for the peripheral model with an addition of $+2.5D$ (PM + 2.5*D*), the central model with an addition of $+2.5D$ (CM + 2.5*D*), the peripheral model with an addition of $+1D$ (PM + 1*D*), the central model with an addition of $+1D$ (CM + 1*D*), and the aspheric model with an addition of $+1D$ (AM + 1*D*).

the CM. The effect of decentration in the AM [Fig. 8(e)] was similar to that found in the CM despite that the variation that occurred in the NS was practically independent of pupil size.

Figure 9 presents the primary spherical aberration values corresponding to the different models and to the two addition values for 5 mm of pupil. We found that regardless of the addition value, the PM was the only model that provided positive values of spherical aberration. For $+1D$ of addition, the CM and the AM presented similar values for negative spherical aberration. Furthermore, for all the models the spherical aberration diminished in absolute value on decreasing the addition.

Finally, we also calculated the value of the RMS of the higher-order aberrations (Fig. 10). The PM was the model that provided the most high-order aberrations, especially for $+2.5D$ of addition. On diminishing the addition, the high-order aberrations also diminished. For $+1D$ of addition, the value found was similar between the CM and the AM, as occurred with the spherical aberration. In specific, when the addition was reduced from $+2.5D$ to $+1D$, the RMS of the PM diminished its value by 64%, and the CM by 56%.

4 Discussion

In this work, we theoretically evaluated three corneal models designed to provide better visual quality both in near as well as in distance vision. With this aim, we optimized the design of each model, calculating the optimal size of the central zone for the two multifocal models as well as the radius and asphericity that characterize each of the surfaces that make up these three models. In addition, we evaluated the visual quality corresponding to each model by the Neural Sharpness and aberrations.

The results show that even using large sizes of the central zone, the multifocal ablation deteriorates the vision for which the central corneal zone had been corrected. Also, it offers only a minor improvement in vision corresponding to the peripheral corneal zone. This result coincides with the results presented by Pinelli et al.,[12] who, despite the use of a central zone of 5 mm corrected for distance vision, reported a significant loss in the contrast sensitivity and an increase in aberrations. However, the efficacy index for near vision was only 0.56 monocularly. In addition, we found that to compensate, a smaller addition permitted the use of a central zone of greater diameter, especially in the CM model. For the CM with an addition of $+1D$, we found an optimal diameter of 2.7 mm, a value very close to the 3 mm normally used in central presbyLASIK.[8,27,28] However, the values that we found for the PM were far lower than those commonly used in the clinic, higher or equal to 3.5 mm.[10–14] Notwithstanding these differences, the results presented in the present work justify the use of a larger central-zone size in the PM than in the CM, as in clinical practice.

Although it is difficult to compare our ablation profiles with those actually used in the clinic because these are usually proprietary, we found a great similarity between our profiles (especially that of the PM) and the multifocal ablation profiles of Telandro[11] on a PMMA plate of a pseudo-accommodative corneal treatment for a hyperopic eye with the peripheral zone corrected for near vision. Our results show that the PM requires a greater ablation depth. This result has been reported by others as one of the main drawbacks of this model.[8,9] Furthermore, the ablation depth significantly increases as the near addition power rises, and thus for large additions, the CM appears to be the most conservative model for the cornea, as others have also pointed out.[9]

In the optimization of the shape of the central zone of the cornea for the three models, the result is a hyperprolate shape (with very negative asphericity values). However, when we analyzed the result of applying the ablation profiles corresponding to each model to determine the general form of the final cornea, the result was a different average asphericity for 6 mm of corneal diameter. Specifically, in the PM, we found a positive average asphericity—that is, the shape of the cornea was flatter in the center and more curved along the periphery. This implies greater power in the periphery than in the center, coinciding with the aim of the PM of creating a zone for near vision on the periphery. Furthermore, we found that the lower the addition, the lower the asphericity was also. As other works have shown previously,[29] a positive value of the corneal asphericity involves

positive values of the spherical aberration and the opposite, as our results corroborate. In the CM and the AM, we found negative spherical-aberration values, whereas in the PM the spherical aberration was positive. Other studies have reported changes to more negative values of the spherical aberration using an ablation model with the center corrected for near vision.[8,9] Although these values are not comparable with ours, Jung *et al.*,[9] for example, found that the coefficient $Z(4,0)$ varied from 0.14 μm pre-surgery to −0.02 μm 6 months after surgery. Also, Alió et al.[8] reported a decrease of spherical-aberration coefficients from 0.41 to 0.36 μm. The fact that the literature does not show positive values for spherical-aberration ablations with the periphery corrected for near vision, as in our PM, is because in most cases analyzed the treatment was made with hypermetropic subjects.[12,13] For correcting a hypermetrope, the curvature of the cornea is increased to raise the power both in the central zone (corrected for distance vision) as well as in the peripheral zone (corrected for near vision). As a result, the ablated corneal zone is made more prolate and increases the negative spherical aberration.[12] The greater spherical aberration extends the depth of focus, favoring the vision for near and intermediate distances.[30,31] It is worth pointing out that one of the limitations of having worked with the Liou-Brennan model is that the initial spherical-aberration values are lower than those of the real eye; nevertheless, this was not relevant to our results, as the aim of this work was to compare the three multifocal models with each other and not to the initial emmetropic model.

The PM provided the highest RMS value of the high-order aberrations. These results agree with those found by Koller et al.[22] also using theoretic corneal models. In that work, the value of the RMS wavefront error found for distance vision was 0.91 μm for a model with a central steep island (i.e., a model with the center corrected for near vision) and 3.54 μm for the cornea with a centered steep annulus (i.e., with a peripheral ring for near vision). Our results also show that the AM is the model with the fewest high-order aberrations. Given that the AM is a model characterized by a continuous conical surface, that is, without abrupt changes of curvature in the central zone, this model would be expected to present the least aberrations.

Despite these differences, we found that on evaluating the NS according to pupil size and decentration, the two multifocal models provided approximately the same values and responded similarly to the variations in the pupil, although opposite. We found that the nasal decentration of the pupil that accompanied the accommodation notably affected the visual quality provided by a given model, especially influencing the vision corresponding to the peripheral corneal zone in the multifocal models. A centered pupil favored the vision corresponding to the central corneal zone, while a decentered pupil favored the vision corresponding to the peripheral corneal zone. However, pupil size played an even more important role in multifocality. Small pupils favored near vision in the CM and distance vision in the PM. On the contrary, large pupils favored distance vision in the CM and near vision in the PM. For the AM, we found that distance vision was very similar to that provided by the two multifocal models, although slightly greater for intermediate pupils. However, this model would provide acceptable near vision only for small pupils (less than 2.5 mm) and for small additions. The aspheric model is recommended in the clinic to correct the nondominant eye for near vision in treatments of monovision.[20] The aim is to create a more curved surface in the central zone and a flatter one in the peripheral zone so that for small pupils the vision would be dominated by this central zone, providing good near vision, while for large pupils the vision would be dominated by the peripheral corneal zone, providing acceptable distance vision. Our results show that this is possible only with compensation of small additions. For large additions, the aspheric model behaves in a completely monofocal way. In addition, it was noted that on increasing asphericity, we worsened only the visual maximums that the model could provide, without this improving vision for other distances.

In all the cases analyzed, we found a clear balance between near vision and distance vision so that whatever was gained in the near vision was lost in distance vision and vice versa. This signifies that although it is possible to improve visual quality in near vision of a subject with presbyopia, this will always bear the cost of worsening distance vision.

5 Conclusion

In this work, we analyzed three new theoretic corneal models based on the ablation techniques applied in clinics to correct presbyopia: two multifocal and one aspheric. For each model, we calculated the different parameters that optimize it for the best visual quality possible both for near and distance vision. The CM model required the least ablated corneal surface area, permitting high addition values, providing more stable distance vision against variation in pupil size, giving more negative values for spherical aberration (thus increasing the depth of field), and furthermore presenting lower high-order aberrations. In addition, if we take into account that the pupil decreases in diameter with accommodation,[32] the CM appears to be the most advisable model for providing multifocality in the cornea. Nevertheless, the fundamental role of the pupil in the resulting visual quality makes it necessary to evaluate the behavior (change in size and decentration) of the pupil of the patient, as well as to study in depth the visual needs before applying this type of surgery.

Acknowledgments

We thank David Nesbitt for translating the text into English. This research was supported by the Junta de Andalucía, Spain, grants P07-FQM-02663 and P06-FQM-01359, and Ministerio de Educación y Ciencia (Spain) grant FIS2009-07482.

References

1. M. Guillon et al., "Visual performance of a multi-zone bifocal and progressive multifocal contact lens," *CLAO J.* **28**(2), 88–93 (2002).
2. J. L. Alió et al., "Near vision restoration with refractive lens exchange and pseudoaccommodating and multifocal refractive and diffractive intraocular lenses: Comparative clinical study," *J. Cataract Refract. Surg.* **30**(12), 2494–2503 (2004).
3. G. Baikoff, "Surgical treatment of presbyopia: scleral, corneal and lenticular," *Curr. Opin. Ophthalmol.* **15**(4), 365–369 (2004).
4. R. H. Keates et al., "Small-diameter corneal inlay in presbyopic or pseudophakic patients," *J. Cataract Refract. Surg.* **21**(5), 519–521 (1995).
5. J. E. Sathl, "Conductive keratoplasty for presbyopia: 1-year results," *J. Refract. Surg.* **22**(2), 137–144 (2006).
6. T. Anschutz, "Laser correction of hyperopia and presbyopia," *Int. Ophthalmol. Clin.* **34**(4), 10–137 (1994).

7. B. Jackson, "Clinical outcomes of presbyopic corrections," presented at the *Fifth Int. Conf. of Wavefront Sensing and Optimized Refractive Corrections*, British Columbia, Canada, pp. 21–24 (Feb. 2004); available at www.Wavefront-Congress.org.
8. J. L. Alió et al., "Correction of presbyopia by technovision central multifocal LASIK (presbyLASIK)," *J. Refract. Surg.* **22**(5), 453–460 (2006).
9. S. W. Jung et al., "Multifocal corneal ablation for hyperopic presbyopes," *J. Refract. Surg.* **24**(9), 903–910 (2008).
10. R. Cantú et al. "Advanced surface ablation for presbyopia using the Nidek EC-5000 laser," *J. Refract. Surg.* **20**, (5 Suppl.), S711–S713 (2004).
11. A. Telandro, "Pseudo-accommodative cornea: a new concept for correction of presbyopia," *J. Refract. Surg.* **20**, (5 Suppl.), S714–S717 (2004).
12. R. Pinelli et al., "Correction of presbyopia in hyperopia with a center-distance, paracentral-near technique using the Technolas 217z platform," *J. Refract. Surg.* **24**(5), 494–500 (2008).
13. A. M. El Danasoury, T. O. Gamaly, and M. Hantera, "Multizone LASIK with peripheral near zone for correction of presbyopia in myopic and hyperopic eyes: 1-year results," *J. Refract. Surg.* **25**(3), 296–305 (2009).
14. M. Gordon, "Presbyopia corrections with the WaveLight ALLEGRETTO: 3-months results," *J. Refract. Surg.* **26**(10), S824–S826 (2010).
15. D. B. Goldberg, "Laser in situ keratomileusis monovision," *J. Cataract Refract. Surg.* **27**(9), 1449–1455 (2001).
16. D. Miranda and R. R. Krueger, "Monovision laser in situ keratomileusis for pre-presbyopic and presbyopic patients," *J. Refract. Surg.* **20**(4), 325–328 (2004).
17. S. Jain, R. Ou, and D. T. Azar, "Monovision outcomes in presbyopic individuals after refractive surgery," *Ophthalmology* **108**(8), 1430–1433 (2001).
18. M. Garcia-Gonzalez, M. A. Teus, and J. L. Hernandez-Verdejo, "Visual outcomes of LASIK-induced monovision in myopic patients with presbyopia," *Am. J. Ophthalmol.* **150**(3), 381–386 (2010).
19. A. Alarcón et al., "Visual quality after monovision correction by laser in situ keratomileusis in presbyopic patients," *J. Cataract Refract. Surg.* **37**(9), 1629–1635 (2011).
20. M. Mrochen, "Hyperprolate corneas for pseudo-presbyopia correction," *Cataract Refract. Surg. Today Eur.* pp. 28–29 (Jan 2009); available at http://bmctoday.net/crstodayeurope/2009/01/article.asp?f=0109_05.php.
21. H. L. Liou and N. Brennan, "Anatomically accurate, finite model eye for optical modelling," *J. Opt. Soc. Am. A* **14**(8), 1684–1695 (1997).
22. T. Koller and T. Seiler, "Four corneal presbyopia corrections: simulations of optical consequences on retinal image quality," *J. Cataract Refract. Surg.* **32**(12), 2118–2123 (2006).http://dx.doi.org/doi:10.1016/j.jcrs.2006.08.038
23. A. Alarcón et al., "Visual evaluation of different multifocal corneal models for the correction of presbyopia by laser ablation," *J. Refract. Surg.* **27**(11), 833–836 (2011).
24. J. D. Marsack, L. N. Thibos, and R. A. Applegate, "Metrics of optical quality derived from wave aberrations predict visual performance," *J. Vis.* **4**(4), 322–328 (2004).
25. L. Chen et al., "Image metrics for predicting subjective image quality," *Optom. Vis. Sci.* **82**(5), 358–369 (2005).
26. L. N. Thibos et al., "Accuracy and precision of objective refraction from wavefront aberrations," *J. Vis.* **4**(4), 329–351 (2004).
27. D. Ortiz et al., "Optical analysis of presbyLASIK treatment by a light propagation algorithm," *J. Refract. Surg.* **23**(1), 39–44 (2007).
28. C. Illueca et al., "Pseudoaccommodation and visual acuity with Technovision presbyLASIK and a theoretical simulated array® multifocal intraocular lens," *J. Refract. Surg.* **24**(4), 344–349 (2008).
29. A. Calossi, "Corneal asphericity and spherical aberration," *J. Refract. Surg.* **23**(5), 505–514 (2007).
30. K. M. Rocha et al., "Expanding depth of focus by modifying higher-order aberrations induced by an adaptive optics visual simulator," *J. Cataract Refract. Surg.* **35**(11), 1885–1892 (2009).
31. R. C. Bakaraju et al., "Depth-of-focus and its association with the spherical aberration sign. A ray-tracing analysis," *J. Optom.* **3**(1), 51–59 (2010).
32. D. A. Atchison and G. Smith, "The pupil," Chap. in *Optics of the Human Eye* **21–29**, Butterworth-Heinemann, Oxford, UK (2000).